12 (2021) 100115

Contents lists available at ScienceDirect

International Journal of Thermofluids

journal homepage: www.sciencedirect.com/journal/international-journal-of-thermofluids

Heat pipe based battery thermal management: Evaluating the potential of two novel battery pack integrations

Hussam Jouhara [a,*], Bertrand Delpech [a], Robert Bennett [b], Amisha Chauhan [a], Navid Khordehgah [a], Nicolas Serey [a], Stephen P. Lester [c]

[a] Heat Pipe and Thermal Management Research Group, College of Engineering, Design and Physical Sciences, Brunel University London, UB8 3PH, UK
[b] Vantage Power, Unit 7 Greenford Park, Ockham Drive, Greenford, London, UB6 0FD, UK
[c] Flint Engineering Limited, The Paddocks, Five Ashes, Mayfield TN20 6JL, UK

ARTICLE INFO

Keywords:
Battery thermal management
Heat mat
Heat pipe
Heat exchanger
Temperature homogeneity
Fast charge

ABSTRACT

Lithium-ion batteries are widely used in high power applications and, with more industries focusing on the electrification of their processes, the need for an effective battery thermal management system is growing. The use of a thermal management system serves multiple purposes such as safeguarding the battery from catastrophic thermal runaway and increasing the lifespan of the battery pack. In the present paper, the thermal management of a sixteen-cell battery module, by two different configurations of a heat pipe based thermal management system, is investigated experimentally. In the first configuration, the module is fixed on top of a single horizontal 'heat mat'. The second configuration consists of the module sandwiched between two vertical heat mats. The comparison of the cooling performances of these two configurations showed their ability to efficiently absorb the heat generated by the cells and maintain their temperatures close to the ideal operating range. During representative cycles of operation, the maximum cell temperature was kept below 28.5 °C and 24.5 °C for the horizontal and vertical heat mat configurations respectively. The cell temperature uniformity across the module stays in a +/-1 °C range, which will reduce cell voltage imbalance, loss of useable capacity and non-uniform ageing. The maximum temperature difference across the height of the cells was 6 °C for the horizontal configuration and 2 °C for the vertical one. The second part of this paper compares the heat removed in both configurations when loaded with a quasi-steady-state heat generation. The third study uses a faster (6C) charge rate during a representative cycle and shows that the maximum temperature stays below 30 °C and 28 °C for the horizontal and vertical configurations respectively.

1. Introduction

The application of Lithium ion batteries is at the epi-centre of the electrification of many industries such as transport and energy. One of the key industries currently moving towards de-carbonisation is the automotive industry by the development of electric vehicles (EV). Currently the European car fleet is expected to reach 19% of EV by 2030. Globally, the trend is similar with the number of EVs expected to increase by 50 times by 2030 [1]. The increase in EV production subsequently means an increased demand in batteries, therefore the production of batteries and thermal management systems will need to increase to meet the demand. The increase in EVs provides an immediate solution to the growing pollution issue prevalent in large cities, the UK in particular has launched a recent incentive to reduce vehicle emissions. The incentive focuses on the development of zero-emission vehicles to accelerate the decarbonisation of the public transport network in England and Wales with a specific focus on the existing bus fleet (5700 vehicles since 2013) [2].

Maintaining the optimum working conditions of the battery is one of the most challenging aims of EV development with a particular focus on battery thermal management systems (BTMS); due to their compact size, extracting the heat efficiently is one of the most challenging limitations. An ideal BTMS aims to reduce the thermal resistance between the cells and the final heat sink with minimal footprint and ease of integration within the vehicle architecture. The BTMS needs to achieve two main aims, the first being the maintenance of the optimum operating temperature for the cells (15–35 °C) [3–5], and the second being to achieve temperature homogeneity amongst the cells. Achieving these aims will

* Corresponding author.
E-mail address: hussam.jouhara@brunel.ac.uk (H. Jouhara).

https://doi.org/10.1016/j.ijft.2021.100115

Available online 25 September 2021

result in significant improvements to the battery's performance and longevity. Low temperatures can cause sluggish electrochemical reactions, resulting in an increase of internal resistance and thus loss of power. The risk of lithium plating at the anode is also greatly increased at low temperatures, which will ultimately reduce cell life. In contrast, elevated temperatures can enable greater power or capacity, as a result of reduced internal resistance, but the drawback is the acceleration of other ageing mechanisms, such as the deterioration of the solid electrolyte interface (SEI) layer at the electrodes. [4]. The temperature inhomogeneity between the cells must also be minimised, in order to reduce cell voltage imbalance due variations in cell internal resistance, which is dependent on the temperature [12,13]. Furthermore, the temperature inhomogeneity within individual cells must be mitigated as they can cause local deterioration on the electrodes due to the uneven degradation and reformation of the solid electrolyte interface that will deteriorate the performance and may result in battery failure [3]. The role of BTMS plays a critical role in the heat removal of EVs, such technologies can delay and even prevent thermal runaway and destruction of the battery cell ('benign failure') [5].

Given the rapid expansion of battery-based technologies, potential solutions for battery thermal management systems are in critical need [6]. One of the most common and inefficient cooling methods is via forced convection by utilising a cooling fluid to flow around the battery cells or battery pack, this causes multiple issues related to battery temperature homogeneity as the fluid increases in temperature as it flows past the cells. By using forced convection and risking non-uniform battery temperatures, the risk of problematic voltage and uneven battery ageing is significant. Multiple technologies have been developed to tackle this issue ranging from PCMs (Phase Change Materials), nanofluids and heat pipes. For instance, Liu et al [14] reported a thermal management system on a 35 kWh prismatic cell battery pack using a liquid based thermal management system. A cold plate made of aluminium channels was fixed to the bottom face of the pack. At a 0.8125C charging and 0.5C discharging rate and with a coolant temperature at 15 °C and 10 L/min, the maximum temperature was maintained under 32 °C and temperature inhomogeneity at 6 °C. The gradient in individual cells was not optimal due to the cooling applied on a single face of the cells. A similar study was conducted by Wiriyasart et al [15], on a mini-channel liquid-cooled battery thermal management system with nanofluid and three different configurations in terms of channel dimensions, flow rate, entrance size to optimize the heat dissipation performance. The model of the battery pack consisted of 444 cylindrical cells. The maximum heat generation of 12.24 W/cell was chosen. The study highlighted that the system reached a maximum water temperature of 50.5 °C but with a maximum difference of 25 °C and with a significant pressure drop [15]. To represent a realistic discharge rate (>10 W/cell), the maximum temperature of 40 °C can be achieved but the inhomogeneity issue is still present. Moreover, the complexity, high cost and leakage risk limit its application. Other efficient technologies such as Phase Change Materials (PCM) have also been investigated as a battery thermal management system. For instance, He et al [16] investigated a system based on a paraffin based PCM absorbed in a skeleton of expanded graphite coupled with a copper foam. The results from the study highlighted a successful integration of the system with an increased mechanical strength of the system. The study highlighted a successful minimum temperature of 48 °C and an overall thermal distribution of 3.9 °C. Although the PCM technology shows potential, the minimum temperatures tested are significantly high especially within the application of vehicle BTMS.

The application of two-phase heat transfer-based technologies as BTMS has expanded into heat pipe technology. The role of heat pipes has been involved in multiple industries ranging from cryogenics to the ceramics industry [17] .Due to their flexibility, passive operation and low maintenance, the role of heat pipes is rapidly expanding within each industry, including BTMS, for instance, Zhang et al [18]. This study used air cooled flat heat pipes to sandwich 5 prismatic cells. At a 4C discharge rate and with air at 25 °C, the maximum temperature was 30.5 °C after 15 minutes. The maximum temperature difference was 3 °C. Gan. et al [19] proposed another heat pipe-based solution for cylindrical cells. The module consisted of a row of 3 cells surrounded by an aluminium spacer cooled on both sides by heat pipes. The final heat sink was water at 25 °C flowing at 3 L/min. During a 5C rate discharge, the maximum temperature of the cells was 33 °C and the temperature difference less than 1 °C. To improve the performance of traditional forced convection methods, a study was conducted by Yuan et al [20], to combine liquid cooling with a heat pipe structure. The study involved a wicked heat pipe where the evaporator section is sandwiched between the battery cells whereas the condenser is attached to a cold plate which contains an internal cooling loop. To validate the heat pipe structure, the test was benchmarked against a typical liquid cooling system with identical operating conditions/ cycles. The outcome from the study highlights similar trends where the discharge temperature increases rapidly. In comparing the two cooling technologies, the maximum temperature for discharge is 36.3 °C and 33.5 °C respectively. The difference in temperature highlights that the battery cannot be cooled effectively which can lead to deterioration. This difference was further noticeable when the evaporator section of the heat pipe was extended to the entire surface of the battery. Several studies have been conducted to determine the optimum heat-pipe/ battery configuration and the optimum contact area. Studies conducted by Yao et al [21], have investigated a rectangular horizontal configuration placed in the middle of two lithium ion battery cells. Similar to the study conducted by Yuan et al [20], the condenser plate is in direct contact with a finned cold plate running a refrigeration loop. Unlike the study conducted by Yuan et al [20], the battery temperature was controllable. This allowed a direct insight into the Coefficient of Performance (COP), when the battery temperature increased from 25 °C to 35 °C, the COP increased from 16.95% to 38.41%, with an exergy efficiency increase by 5%. The arrangement of horizontal heat pipes has also been investigated by Behi et al [22]. The study involved individual flat heat pipes in between two battery cells, with the condenser section being located in ambient conditions. Similar to previous studies, the cell temperatures exceeded 34 °C, but with the addition of the heat pipe system, the battery temperature reduced to 22 °C. Alihosseini and Shafaee [23], conducted a similar study to investigate the placement of wicked single flat heat pipes between two battery packs, with the condenser section being located in water at a set temperature of 22 °C. The results highlight that during operation the battery temperature was exceeding 36 °C, but an increase in the condenser section flow rate reduced the cell temperature significantly to 29 °C. From the studies it is evident, that heat pipes can play a significant role within BTMS systems. Jouhara et al [24] developed a new flat heat pipe design optimized for high thermal performance, compactness and ease of use in battery thermal management. A module consisting of sixteen prismatic cells was put to the test with a representative cycle ending with a 10-minute 4C (3.5 kW) fast charge. The cell temperatures were maintained in a 17–27 °C range with excellent temperature homogeneity across the module (+/-1 °C) and 6 °C maxi mum temperature difference within a cell. The coolant was water at 15 °C flowing at 10 L/min in the water jacket condenser of the heat mat. Since the cooling was only applied to the bottom face of the module, the internal thermal resistance of the cells prevented the hottest part of the cells (at the top close to the terminals) from benefiting from the enhanced heat transfer of the heat mat.

This paper compares the thermal performance of vertical and horizontal configurations of the novel heat mat flat heat pipe technology. The study demonstrates the influence of the configuration on the thermal performance of a Li-ion battery pack and will indicate how through cooling of battery cells, life cycle increases and efficiency improvements can be achieved.

2. Methodology

2.1. Description of battery module

The tests carried out in this paper were conducted on a prototype battery module designed and built by Vantage Power, for potential application to EV buses. The module consisted of 16 prismatic LTO cells from a leading cell manufacturer. Each cell has a nominal capacity of 23Ah and a nominal voltage of 2.3 V. The battery itself is capable of approximately 10,000 charge cycles and continuous charge rates above 4C.

Fig. 1 shows the two configurations used in the tests. Fig. 1a consists of a single horizontal heat mat flat heat pipe, under the bottom side of the module. The module is fixed by two brackets on the side and secured along the length of the heat mat to ensure full contact. Fig. 1b represents the vertical configuration. To ensure full contact and optimised heat transfer, a thermal interface material was applied between the heat mats and cell surfaces.

2.2. Test bench setup

Testing of the battery modules and heat mats was conducted using Vantage Power's testing bench on their dedicated battery test enclosure as shown in Fig. 2. The modules were supported by foam polystyrene blocks to provide a level of insulation between the test rig and test bench.

Each cell's surface temperature was data-logged in two of three positions, as shown in Fig. 2B, dependant on the heat mat configuration. The highest cell temperatures were expected to occur at the location between the positive and negative tabs of the cell (T17), therefore the temperature at this location was monitored for both configurations. The temperature at the T17 location was measured by a 10 K NTC thermistor, which was read by a module control board (MCB) with 1 °C resolution.

For the horizontal heat mat configuration, the cell temperatures were also monitored at the T10 location; on the lower part of the side face, 30 mm above the bottom edge (see Fig. 2C). For the vertical configuration, due to the presence of a heat mat on each side of the module, the T11 location, in the centre of the bottom face, was used. (see Fig. 2D). T-type thermocouple sensors were used to measure the T10 and T11 temperatures and were chosen for their size factor, accuracy, temperature range and fast response. The test bench and battery management system were controlled and data-logged from a National Instruments cRIO-9068 chassis, multiple C-series I/O modules with a custom LabView program.An EA-PS 8080–340 DC power supply and an EA-EL 9080–400 electronic load, controlled via CAN, were used to charge and discharge the battery module. The electrical connection between the battery module and the power supply/electronic load was controlled by a custom-built contactor box which also contained an insulation measurement device (IMD) and a high sensitivity current and voltage measuring device (IVT).

3. Results and discussions

3.1. Investigation of cooling performance of representative cycle tests

Fig. 3 shows the module's DC power, state of charge (SoC) and the calculated heat generation during a discharge-charge cycle representative of a real-world operation. The cycle is intended to represent the operation of the module in an opportunity-charged electric bus application. The cycle consists of four iterations of ~45 minutes of charge-depleting operation, representing a bus driving in an urban environment, followed by rapid charging at a rate of 4C. The heat generation shown in Fig. 3 represents Joule heating, calculated from the measured current and maps of the cells' internal resistance as a function of temperature and SoC. During the charge-depleting part of the cycle, the greatest heat generation was caused by some prolonged periods of high-power discharging (after ~20 minutes) and also at towards the end, as a result of an increase in the cells' internal resistance at low SoC. These peaks of heat needed to be removed quickly to avoid accumulating temperature rises in the cells. From Fig. 3, it can be observed that the battery's state of charge decreases rapidly as the heat generated by the module increases.

Fig. 4 shows the evolution of the average temperatures at the top of the cells (T17) and at the bottom (T11) or the closest available position (T10) in the case of the horizontal mat. As illustrated, it can be explained that in the vertical configuration, the temperature at location T17 decreased by 4 °C at the end of the last charge when the maximum temperature was reached. The average temperatures at the top and bottom of the cells were shown to be very close and within 0.6 °C. It should be noted that during the entire test, the module stayed within an ideal temperature range of 18 to 25 °C. In the horizontal configuration,

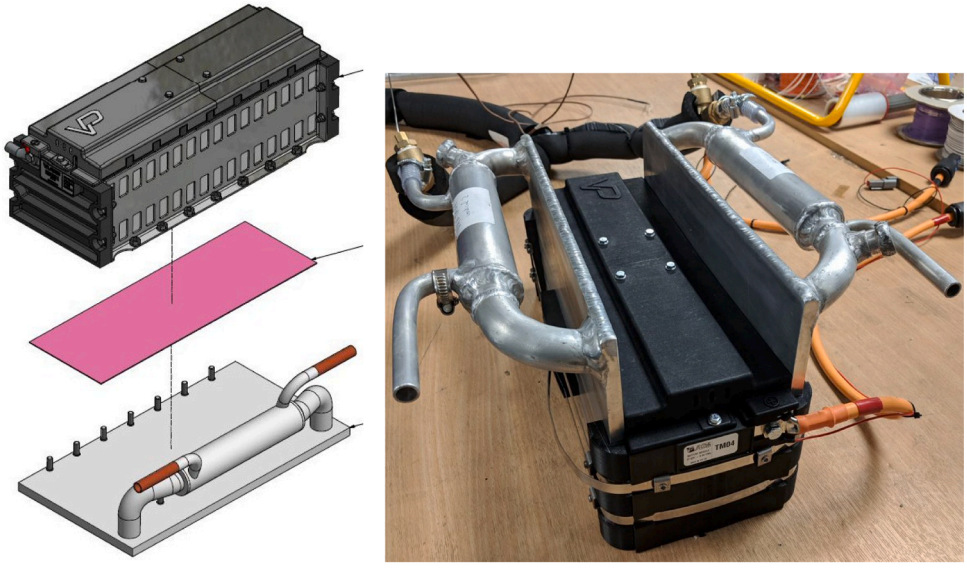

A B

Fig. 1. (A) Horizontal mat configuration, (B) vertical mat configuration.

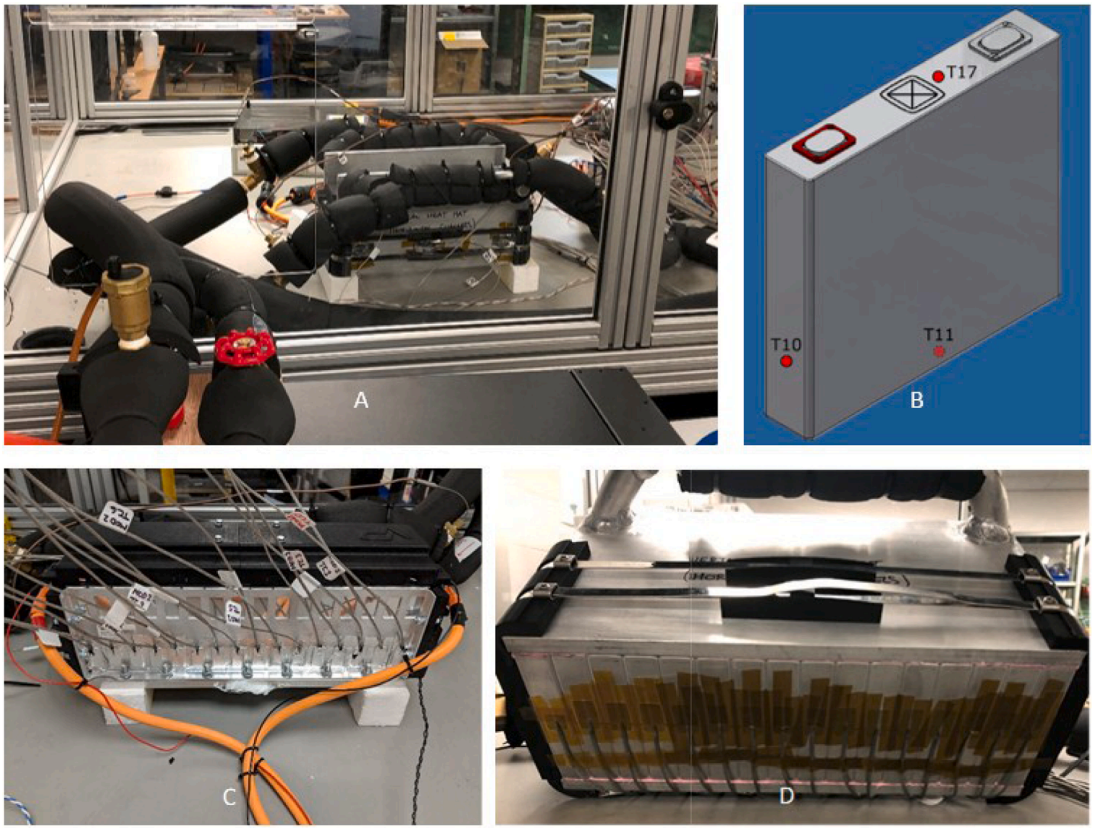

Fig. 2. (A) Test bench overview. (B) test cell (C) Horizontal configuration (d) vertical configuration.

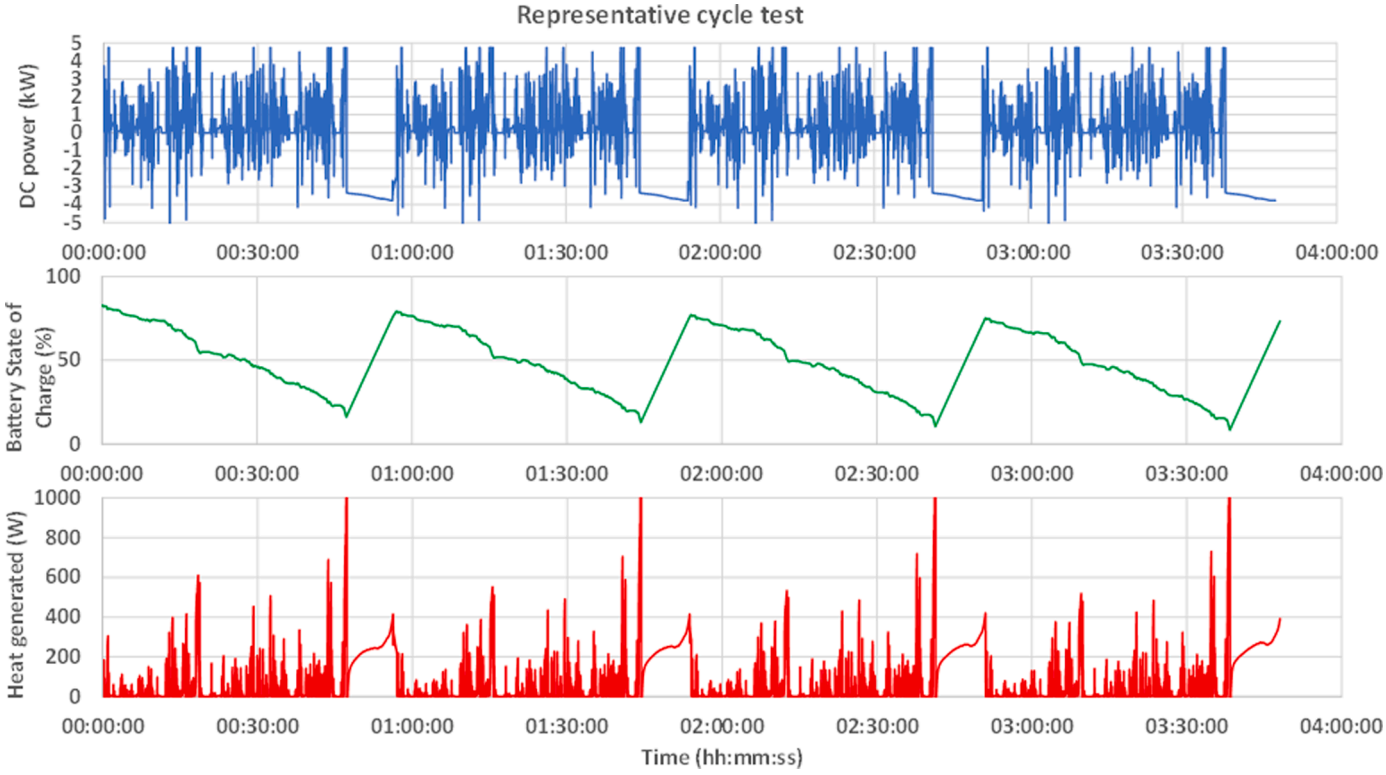

Fig. 3. (a) Module DC power of the representative cycle, (b) evolution of the state of charge, c) calculated heat generated by the module.

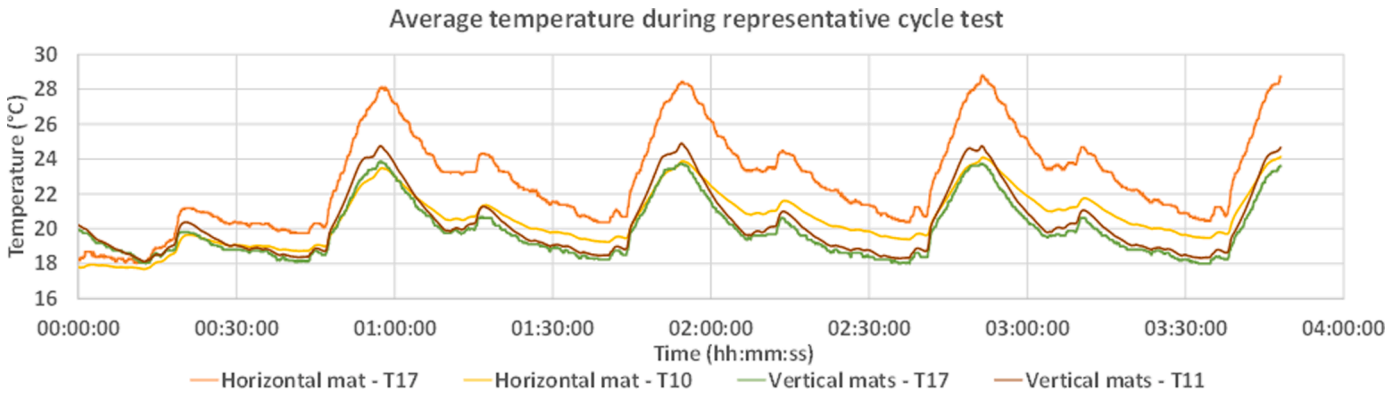

Fig. 4. Evolution of the average temperatures at the top of the cells (T17) and at the bottom (T11) or the closest available position (T10) in the case of the horizontal mat.

this range was shown to be slightly wider, between 18 and 29 °C. But in both cases the temperature of the pack stayed within the recommended range of the cell manufacturer. Furthermore, it took between 7 and 9 minutes for the temperature of location T17 on the horizontal mat to fall below 25 °C after the end of the recharge. During this time, it was noted that the cell operates above the optimal temperature potentially causing a loss of capacity through accelerated ageing over time. It should be noted that the coolant used in the experiment was chilled water flowing at 9.5 L/min and 15 °C through the condenser of the heat mats.

Subsequently, it was observed that a faster temperature rise occurred corresponding to the long accelerations and regenerative braking in the middle of each cycle and near the end before the charge. Furthermore, it was discovered that the average temperature of the heat mat in both orientations increased by no more than 1 °C which was considered to be in an acceptable range. Nevertheless, for the horizontal orientation, it was observed that a very slow rise in temperature of about 0.2 °C occurs between each of the passing cycles. Having mentioned that, this effect completely disappears when the heat mat was used in the vertical position with the temperature consistently fluctuating between 18.0 °C and 24.6 °C.

3.1.1. *Cell temperature homogeneity length-wise*

Fig. 5 represents the temperature homogeneity recorded across the module at the T17, T11 and T10 positions.

It was observed that the temperature readings from the thermocouples used in both cases are rather homogenous, with the difference of results between 0.5 °C and 2 °C degrees around the cells. As mentioned before and unlike other thermal management methods, the cooling through the heat mat is applied in a homogenous manner to the surface of the cells. This means that the isothermal behaviour of the heat mat enables the temperature to be equilibrated everywhere in the module. In contrast for example in di-electric oil baths or forced airflow cooling systems, the temperature of the battery progressively increases along the path of the heat sink fluid, since the temperature of the working fluid increases as it absorbs the energy of the battery. Such temperature differences will potentially result in dissimilar discharging rates at different locations in the battery module, since the internal resistance of a cell is closely related to its temperature. When operating at too low or too high temperature, the charging and discharging rate can be affected. This will result in a voltage unbalancing effect that reduces the total capacity of the battery [7–14]. To protect against permanent losses of capacity, the cells are not allowed to discharge under a certain voltage. In practice, when the first cell reaches this low level, the entire battery is switched off even if some cells were still above the aforementioned threshold. In the long run, keeping the battery pack at a uniform temperature reduces the risk of rapid ageing of the hottest cell which in return will result in an increase of the total life span of the entire battery.

3.1.2. *Temperature difference with height*

The maximum temperature differences across a cell height recorded for both the horizontal and the vertical configurations of heat mat are presented in Fig. 6.

It can be seen from the results, in the horizontal configuration a rapid increase in temperature at the top of the cell is observed which coincided with the recharge period of the representative cycle. At the same time, it was discovered that the bottom of the cells stays at a cooler temperature due to the direct contact and conductive cooling by the heat mat on the battery cells. Having indicated that, the heat at the top of the cell was found to be harder to extract, mainly due to the fact that the heat mat is directly placed at the bottom of the battery pack. Having noted that,

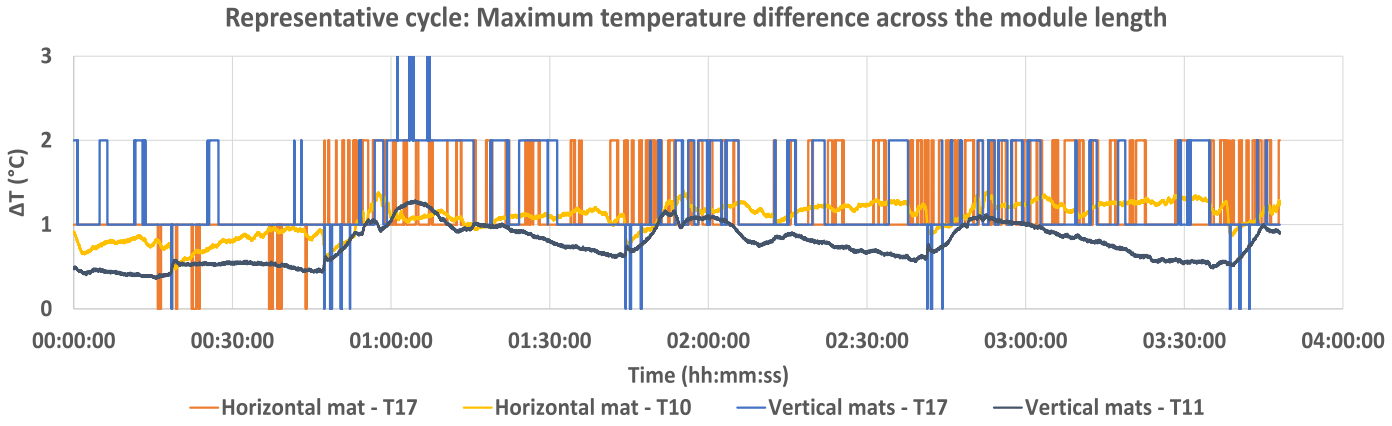

Fig. 5. Module temperature homogeneity, during the representative cycle test. Data are shown for each of the two thermal management systems that were tested.

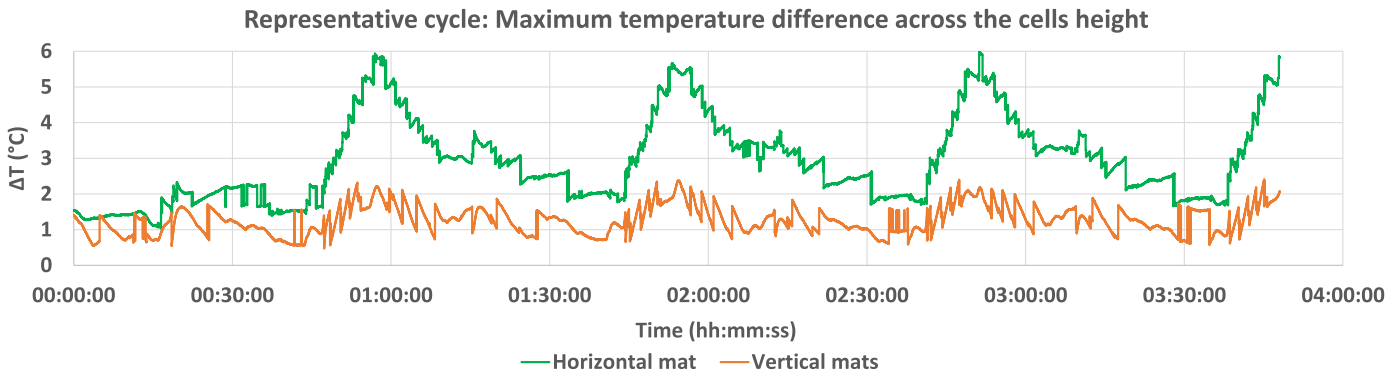

Fig. 6. Maximum temperature difference recorded between the top and the bottom of the cells during the representative cycle test.

however, the temperature difference in this configuration never exceeded 6 °C at its peak. It should be explained that this difference in a particular cell is not as critical as the thermal unbalance between cells, as it does not directly lead to a change in discharging or charging rate. This can nevertheless affect the local resistance inside the cell volume which in turn can participate in raising the total average temperature of the cell and thus lower its capacity.

In the vertical configuration, on the other hand, heat mats were placed on each side of the cells. Having noted that, the temperature of the heat mat was still found to be homogenous along the height of the side of the cell. In fact, and as demonstrated by Fig. 6, a maximum temperature difference of 2.4 °C was observed with a more uniform temperature distribution along the battery pack when compared to the horizontal configuration. The vertical placement of the heat mat also resulted in a reduction of temperature gradient with height, since the relative distance to any point of the cell to the heat mat was constant along the height. Furthermore, it was discovered during the experiment that the hottest parts of the cells are actually the two electrode tabs at the top of the battery pack which were not in contact with the heat mat.

3.1.3. *Temperature difference across heat mat evaporator*

Fig. 7 shows the maximum temperature differences for the horizontal and vertical configurations as recorded at different strategic locations along the heat mat.

A good indicator of the heat mat operation is to check if the temperature along the surface of the heat mat is truly homogenous. As with all saturated two-phase heat transfer methods, a difference in temperature indicates a disruption of the heat transfer. If the heat cannot be rejected effectively to the ultimate heat sink medium, the temperature of the aluminium body of the heat mat quickly rises towards the temperature of the cell in contact. As can be seen from Fig. 7, it has been shown that the temperature difference along the surface of the heat pipe during most of the test was kept below 1 °C, which indicates that the heat mat is operating as expected while offering a low thermal resistance. Having established that, during the intensive heat generation of the recharge, the second vertical heat mat showed that the temperature difference is approximately 2 °C. This value however is not critical and can be explained by the different filling ratio of working fluid in the two vertical heat mats that were tested. To mitigate this effect, a larger filling ratio can be chosen during the design phase.

3.1.4. *End cell temperature distribution*

Fig. 8 shows a detailed view of the temperature of the module after 4 representative cycles at the hottest point at the end of the last charge.

As illustrated, the temperature distribution is found to be homogenous across the length of the module in both cases. When the battery pack is uncooled, the temperatures tend to form a bell-shaped curve with the end cells at lower temperature due to the convective cooling by the surrounding air. This mode is however insignificant compared to the isothermal self-balancing effect of the heat mat. As demonstrated, the vertical configuration performs better by forcing the temperature to be within 2 °C across the height while at the same time reducing the maximum temperature by almost 6 °C as shown by the results from cell 12 for example.

It should be mentioned that without cooling or if a cell locally reaches a high temperature (i.e. in case of a cell defect), it risks a catastrophic self-accelerated degradation called thermal runaway. This will lead the cell to potentially reach temperatures as high 900 °C while releasing large amounts of toxic flammable gases. The heat mat rapid cooling homogenous temperature can in this regard be an ideal candidate for battery thermal management. The technology can prevent the thermal runaway from propagating to neighbouring cells and keep the incident isolated by slowing down the reaction.

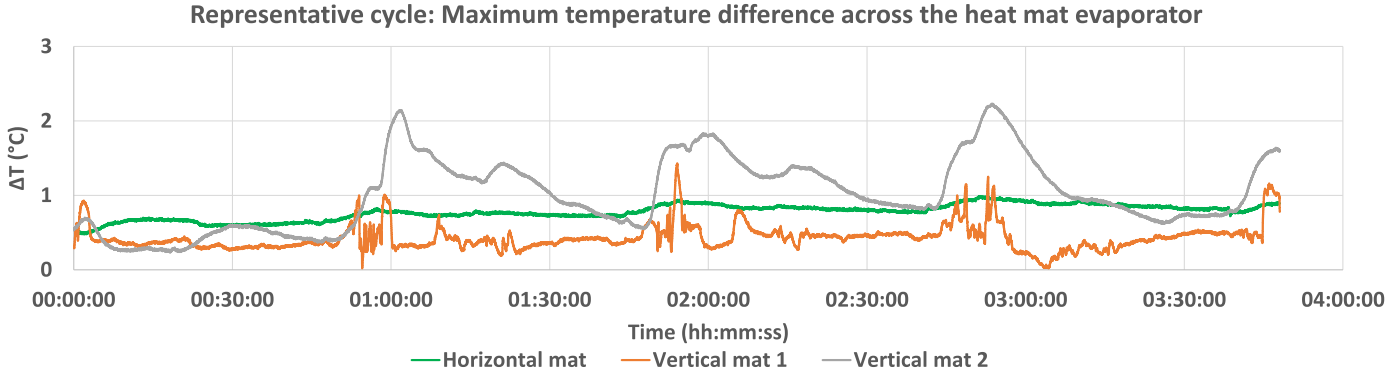

Fig. 7. . A figure of the maximum temperature difference across the surface of the three heat mats during the representative test.

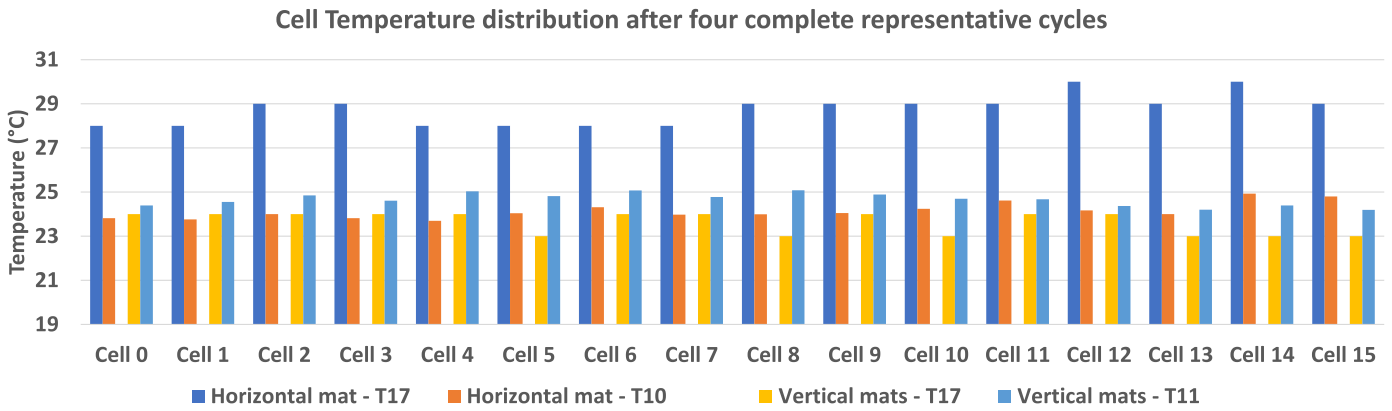

Fig. 8. Module temperature distribution, at the end of four complete representative cycles. Data are shown for each of the two tested thermal management systems.

3.2. *Constant heat generation (10 s pulses)*

In order to assess the performance of these new configurations, tests were conducted at constant heat generation to investigate the behaviours of the heat mats in a worst-case scenario. A similar approach was done by Jouhara et al [24] where the test involved the rapid charge and discharge of the battery module at a 10 s pulse and 50% SoC for 52 min. The operation of the battery cells highlighted a constant heat flux on the evaporator surface of the mats at an average power of 90 W, as can be seen in Fig. 9. As presented by Fig. 9 (a), the state of charge of the battery increases gradually from about 40%, while the battery DC power rapidly changes through the experiment. Having mentioned that and as can be seen from Fig. 9 (b), when the charging cycle is less rapid, the state of charge remains almost constant at about 40%.

3.2.1. *Horizontal mats*

As presented by Fig. 10, the module heat generation during the constant heat generation test on the horizontal configuration slightly decreases by about 10 W before rapidly increasing to 120 W. Having indicated that, the generated amount of heat was expected to stay on average at about 90 W. The impact of the constant heat flux through the heat mat can be seen in Fig. 11. The heat mat increases in temperature until a steady state is achieved after 30 minutes. In the case of the horizontal heat mat, the maximum evaporator temperature reaches 16.4 °C while the temperature difference between the water inlet and outlet is 0.15 °C. The battery temperature reached a maximum of 20.3 °C for T10 and 25.0 °C for T17. The horizontal mat managed to maintain the temperature of the battery under the safe operating value. However, the battery temperatures within the cells were not optimal.

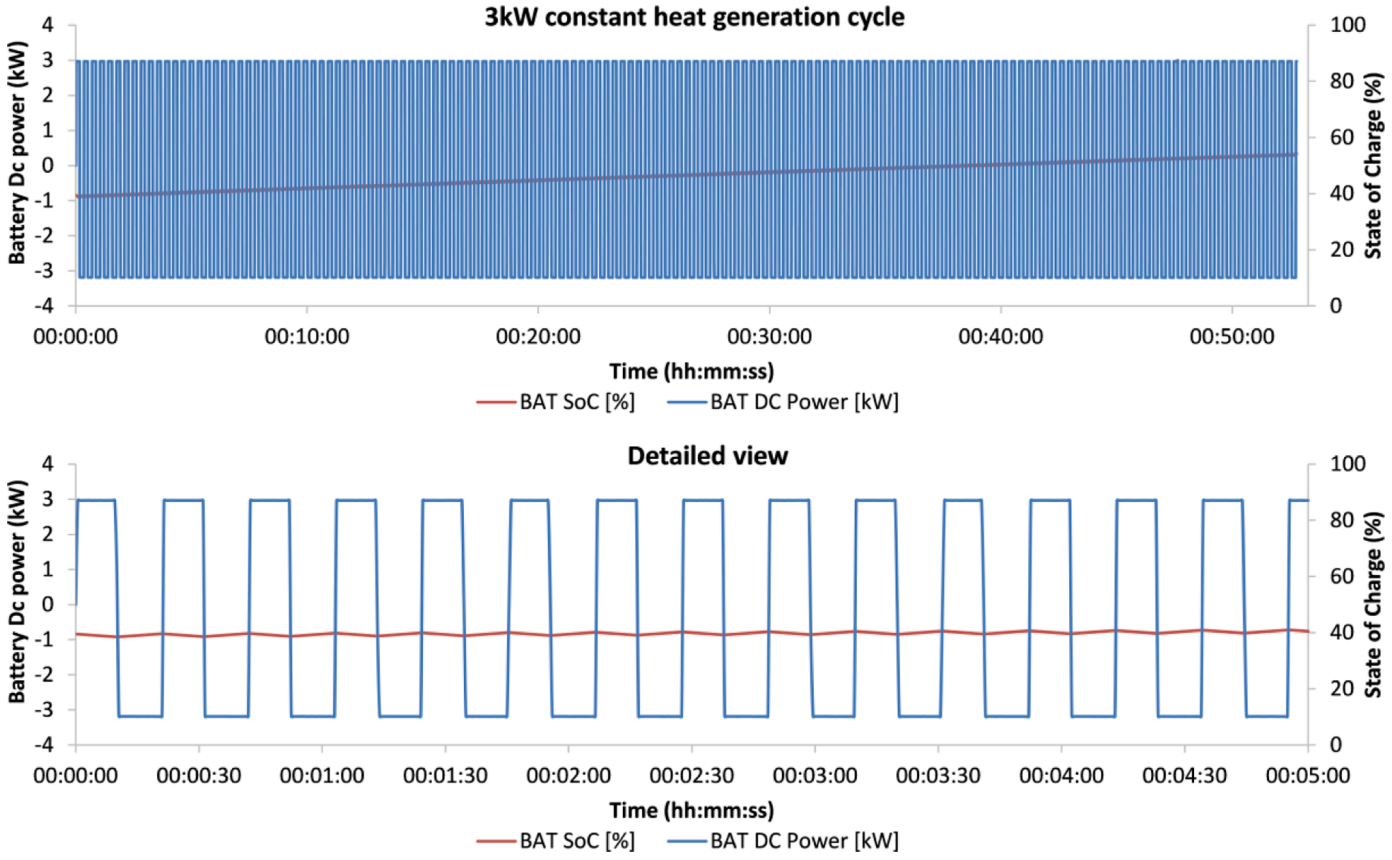

Fig. 9. (a) Module DC power; (b) state of charge for the constant heat generation duty-cycle with detailed view. Negative values of DC power represent charging and positive values represent discharging.

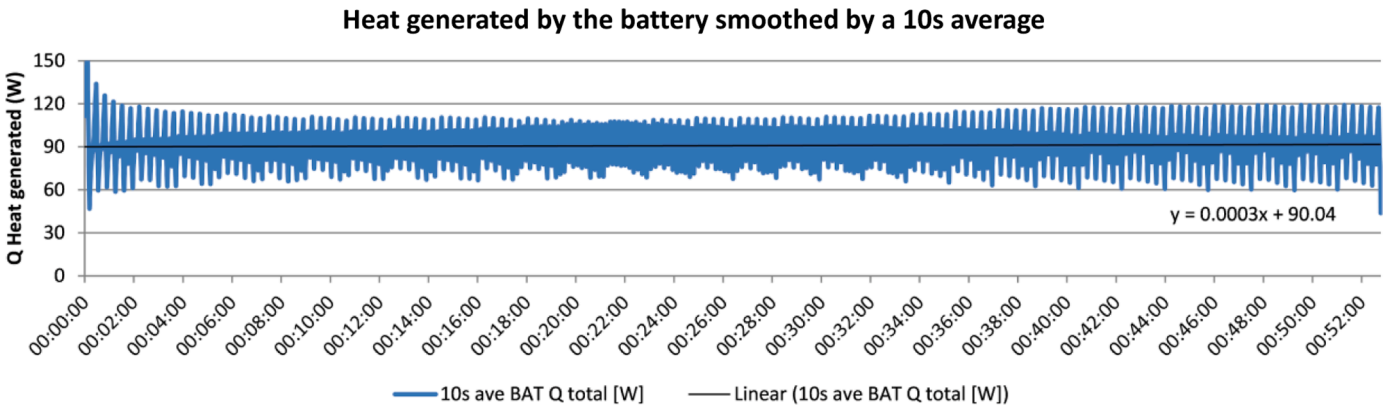

Fig. 10. Module heat generation during the constant heat generation test on the horizontal mat. (For ease of viewing, the data have been smoothed using a 10 second moving average).

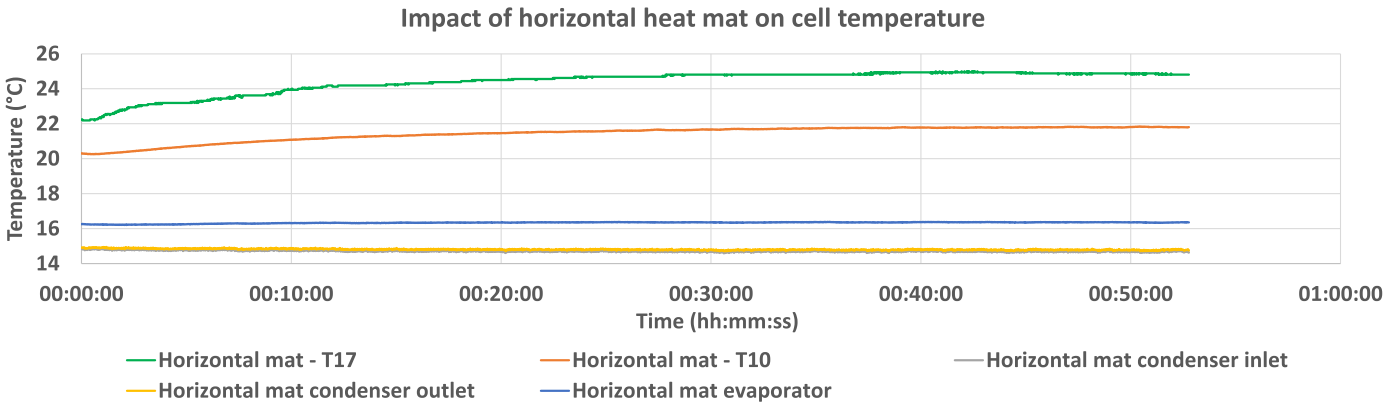

Fig. 11,. Average temperature at the top and bottom of the cells, of the heat mat and water temperatures.

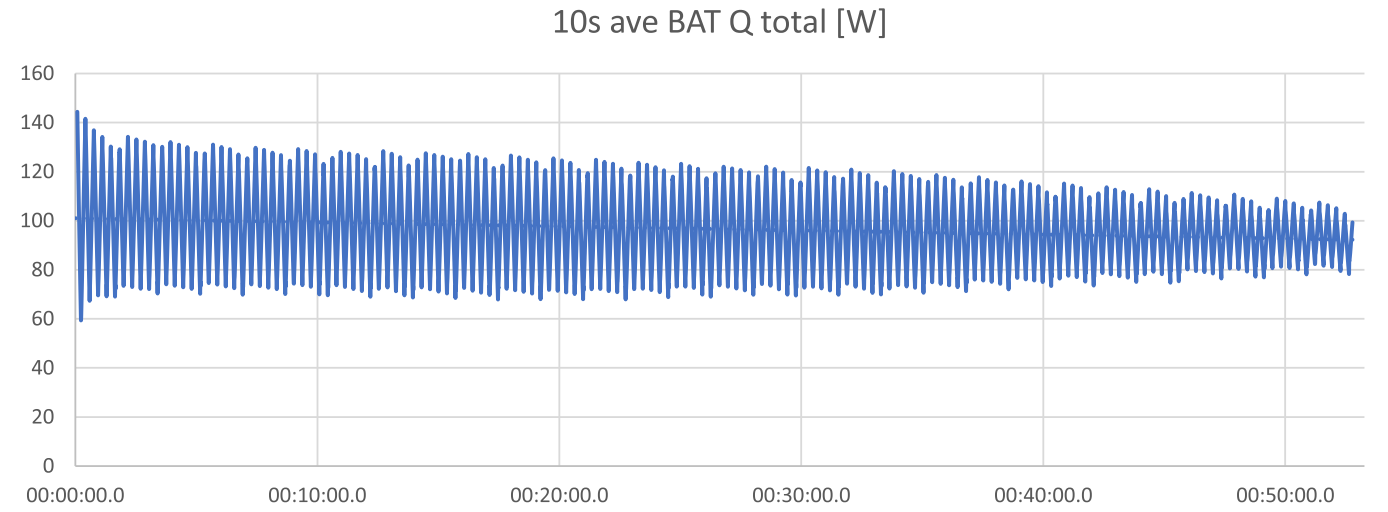

Fig. 12. Estimated module heat generation during the constant heat generation.

3.2.2. *Vertical mats*

A similar approach was made for the vertical mats. A higher heat transfer rate was applied to the battery at 100 W as shown in Fig. 12. As presented, the estimated heat generation of the module throughout the experiment decreased substantially from a maximum of 140 W to about 110 W. Fig. 13 shows the temperature distributions of the mats and the battery pack for a vertical configuration. It can be seen that maximum battery temperatures of 21.5 °C and 21.3 °C are reached for T11 and T17after the steady state is achieved. A better uniformity in the temperature of the battery cells is achieved with the vertical mats. The maximum temperature difference between the water inlet and outlet is 0.19 °C for vertical heat mat 1 and 0.29 °C for vertical heat mat 2. It can be noted that the temperature of the evaporator section for vertical mat 2 is much higher than for vertical mat 1, 19.7 °C and 17.1 °C respectively. This effect can be caused by a difference in inclination between the two mats or in the filling ratio in the evaporator section of the heat

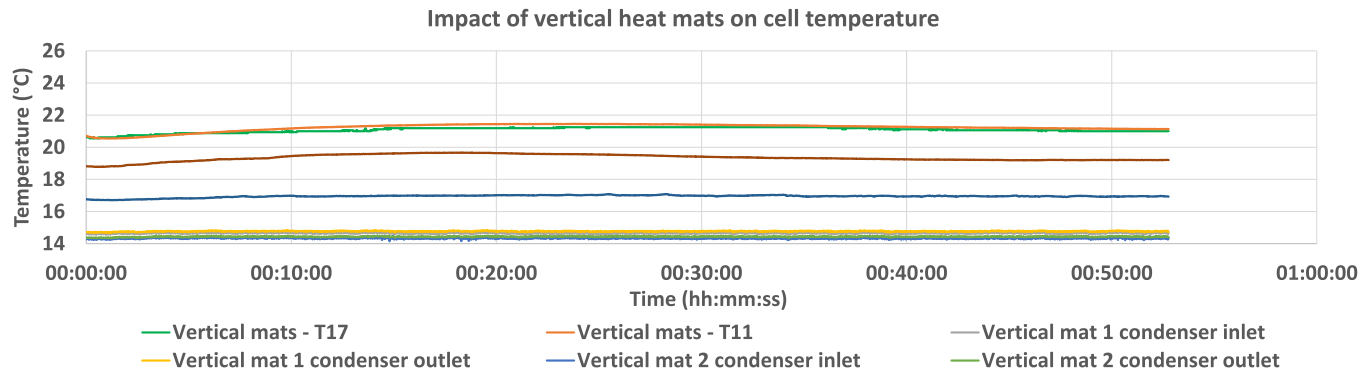

Fig. 13. Average operational temperatures of the mat and the cells.

mat.

3.2.3. Discussion

It can be seen that the temperatures of the battery at a constant heat input are much lower for the dual vertical mat than for the horizontal system. This is mainly driven by the heat transfer surface area for each Heat Mat. Indeed, the heat transfer area of the vertical mats is larger than for the horizontal one, hence an increased heat transfer rate will occur. The position of the mat on the side will also have an impact on the increased temperature control of the battery as the heat generated by the battery is in the centre and top rather than at the bottom. It can be concluded from this results that the vertical mats will provide an enhanced performance compared to the horizontal mat.

3.3. Investigation of the battery module reaction to a higher power charge

The representative cycle test was repeated on the vertical mat configuration with a higher charge rate to investigate the effect on the heat mat behaviour and the module temperatures. A higher charge rate will imply higher heat generation, thus higher heat rejection. However, faster charging can reduce charge time and increase availability of the vehicles.

3.3.1. Representative cycle test 6C/4C charge

The innovative battery thermal solution was exposed to a similar charge and discharge cycle as described in the previous test. An illustration of the charging discharging cycle can be seen in Fig. 14. By increasing the charging rate from 4C to 6C, a notable reduction in charging time was achieved, reducing the charging time by 26%. However, the heat generated by the battery increased from 400 W for a 4C charge rate to 665 W for a 6C charge rate. This extra heat generated by the battery will need to be rejected by the vertical mat to avoid any overheating of the battery.

3.3.2. Average temperature

The evolutions of the battery temperatures during the higher charge rate test are presented in Fig. 15 for the top and bottom of the cells. A similar temperature profile for the 6C and 4C charging and discharging rate can be seen. During the 6C charge, the average temperature of the cells reached a maximum of 29.9 °C, whereas for the 4C charge it only

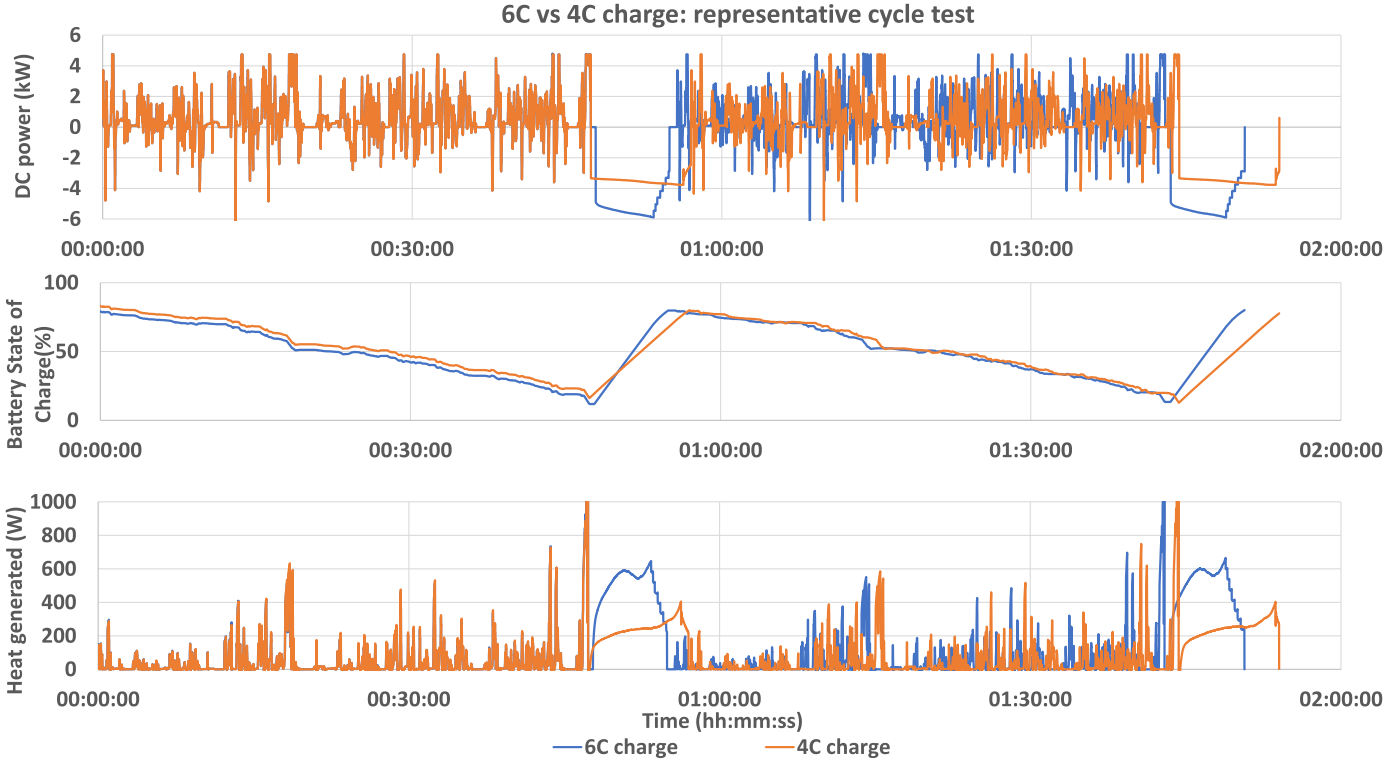

Fig. 14. (a) Module DC power of 4C and 6C representative cycle, (b) State of charge, (c) calculated heat generated by the module.

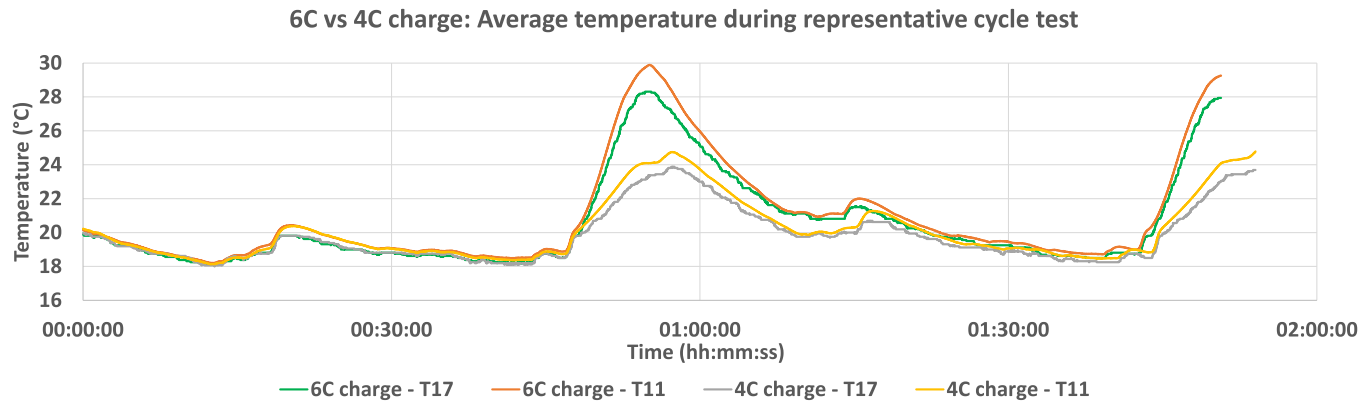

Fig. 15. Average temperatures at the top of the cells (T17) and at the bottom (T11) for 4C and 6C charge.

reached a temperature of 24.8 °C. In the case of the 6C charge, the cells temperatures remained above 25 °C for 10 minutes. At the end of the 6C charge, the cell temperature decreased to reach a similar temperature to the 4C charge after 20 minutes. It can also be noted that the module maintained the cell temperature in the recommended range even with a faster 6C charge. With respect to the maximum temperature, the safety and longevity of the cells is ensured by the vertical heat mat configuration.

3.3.3. *Cell temperature homogeneity length-wise*

Fig. 16 illustrates the homogeneity of the module over the 6C and 4 C charge cycle. It can be seen that the temperature difference of the module is maintained below 3 °C at the top of the battery and 2 °C at the bottom. It can be concluded that the homogeneity length wise is not affected by the charge rate increase from 4C to 6C rate as similar behaviours for the two charge rates are observed. At the bottom of the cells, the maximum temperature difference observed between the rates was measured at 0.5 °C. Thus, there is no observable consequence from the faster charge on the loss of capacity from voltage unbalancing since the temperature variation throughout the battery pack is negligible. The temperature distribution within the cell also needs to be as uniform as possible to avoid a fast ageing of the battery pack.

3.3.4. *Temperature difference with height*

Fig. 17 illustrates the maximum temperature difference within a cell at T17 and T11. The peak difference of the two temperatures over the 4C and 6C cycle is less than 1 °C. The maximum variation in both charge rates does not exceed 3 °C. Hence, the higher charge rate does not affect the maximum temperature gradient of the cells. Most of the heat during faster charging will occur at the cell's tabs located on the top of the battery; it can be seen that using the vertical mats, the temperatures are still well distributed across the cell. This ensures the protection of the cells as the effect of the local temperature variations on the cell's internal resistances and the subsequent ageing processes are reduced.

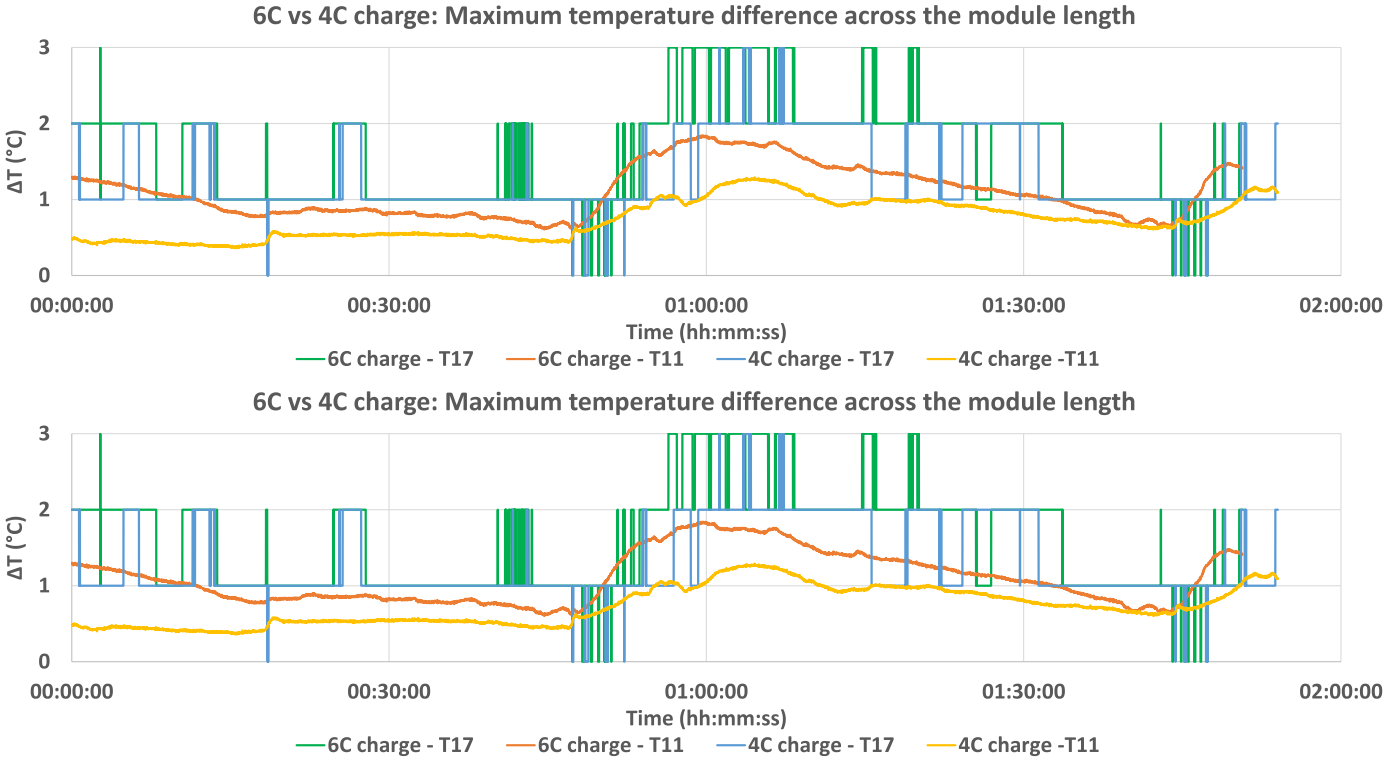

Fig. 16. Module temperature homogeneity for each charging rate

To ensure that the cells within the battery pack will be able to sustain repetitive charging and discharging cycles, the homogeneity of the battery pack temperature need to be ensured.

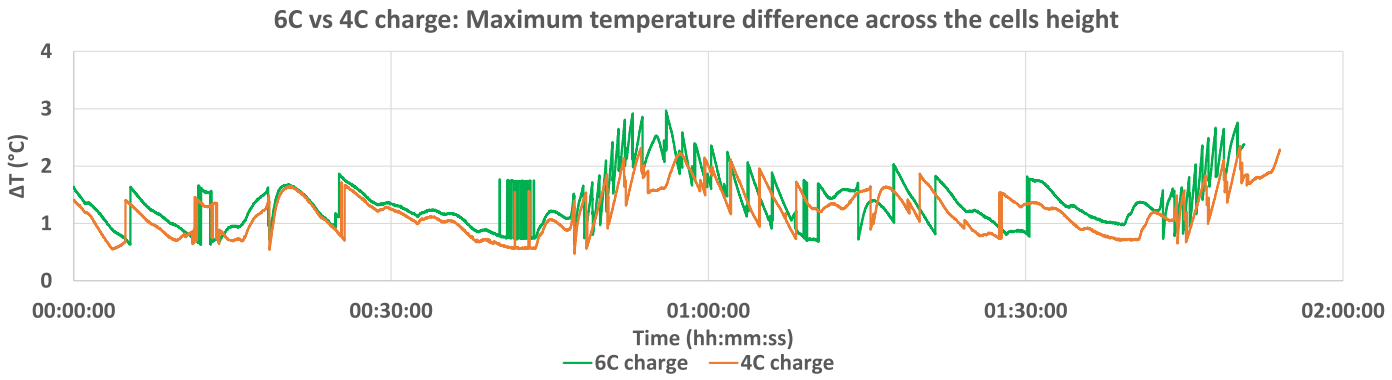

Fig. 17. Maximum temperature difference between T17 and T11 for the 4C/6C charging rates.

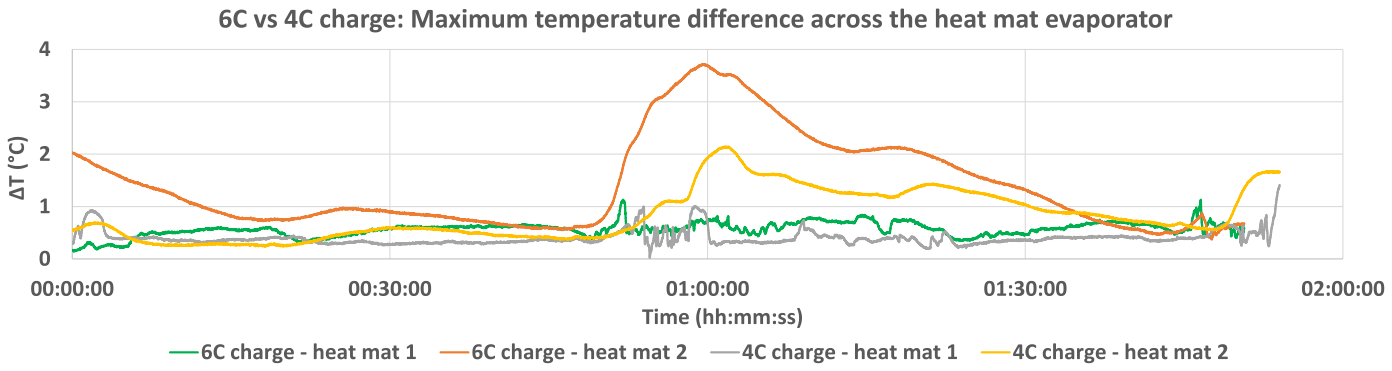

Fig. 18. Maximum temperature difference across the surface of the heat mats during the 4C/6C charging rates.

3.3.5. *Temperature difference across heat mat evaporator*

Fig. 18 illustrates the evolution of the temperature at the evaporator section for each mat under each charge rate for two cycles. Heat mat 1 performed well during the experimental test under both charge rates. A good homogeneity of temperatures across the mat was demonstrated with a maximum temperature difference below 1 °C during the two complete cycles. Variations in Heat Mat 1 temperature are mainly due to local increases of heat flux due to the charge and discharge rates of the battery cells. It can be noted that in the case of Heat Mat 2, the temperature distribution across the evaporator section exceeded the value of Heat Mat 1. The maximum temperature variation across the evaporator section was achieved during the fast charge at 6C for at a maximum of 3.7 °C. This can be due to local dry out of the evaporator section, potentially due to a lower working fluid amount or a different inclination. It can also be caused by a faulty battery that will generate higher local heat flux, thus increasing the temperature of the heat mat surface. However, the temperatures of the cells remained quite uniform.

3.3.6. *End cell temperature distribution*

In order to highlight the temperature distribution of the cells across the battery pack, the temperatures of each cell at the top and bottom have been plotted for the two charge rates at 4C and 6C at the end of the last charge cycle. These temperatures are illustrated in Fig. 19. It can be seen that for both charge rates, the temperatures across the battery are quite uniform. Typically it would be expected that the cells located on the ends of the module would be significantly cooler than those towards the centre of the module, as a result of increased natural convection and radiation at the ends of the module. A noticeable difference can be seen between the top and the bottom of the cells. As expected, the battery cell temperatures are higher for a higher charge rate but remain within the safe boundaries of use for this type of cell.

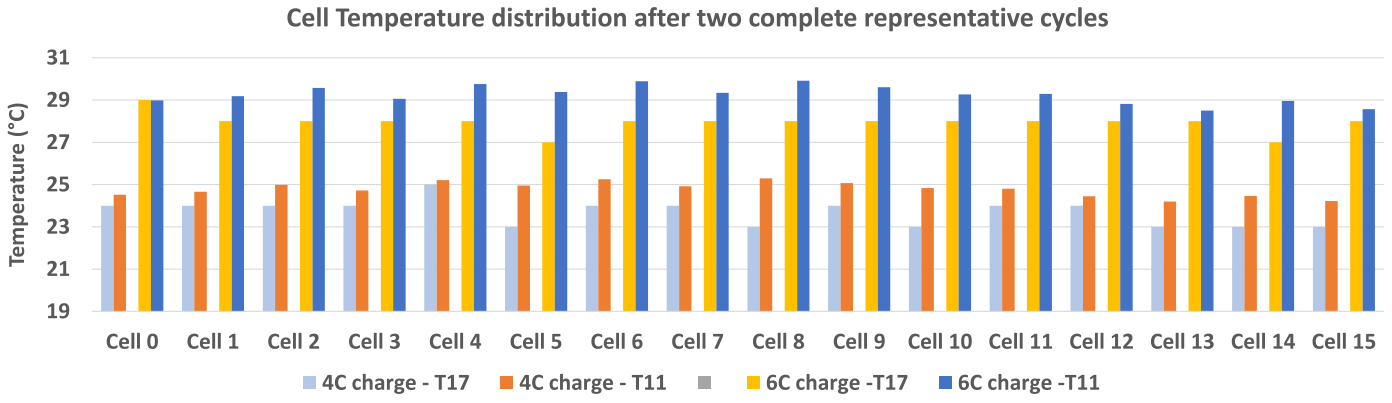

Fig. 19. Module temperature distribution, at the end of two complete representative cycles for each charging rate.

4. Conclusion

This research presented the use of a Heat Mat as a battery thermal management solution, two different module integrations were studied and compared. A battery located on top of a horizontal heat mat showed significant cooling performance, by keeping the cells in an 18 °C to 29 °C range on average. The technology shows significant potential as the maximum vertical temperature difference reached only 6 °C. This difference is attributed to the battery cooling method: cooling from the base means cooling from the face of the cell farthest from the hottest part (electrode tabs). Therefore, the intrinsic thermal resistance of the cells is the main factor contributing to the observed temperature gradient. The second module integration considered sandwiching the module between two heat mats. This configuration increases the number of parts of the system but results in an improved cooling performance to a level yet unobserved in battery thermal management for such compact systems. The temperature range was 18 °C to 25 °C and the temperature inhomogeneity was reduced to 2 °C both across the module and across the cell height. These unprecedented results demonstrate that the heat mat cooling system is amongst the best solution for battery thermal management performances. Having multiple heat mats between the modules in the battery pack will increases the safety of the individual batteries by the principle of redundancy. As each cell is in contact with two cold sources, the thermal resistance is approximately halved. In case of failure of one of the heat mats, one mat is enough to cool the cell enough to avoid overheating or catastrophic thermal runaway. The study proved the possibility of charging the battery with a 50% increased rate, while maintaining the temperature within the recommended range and without affecting the temperature distribution throughout the module and within each cell. The vertical setup offers sufficient heat transfer to cancel any temperature rise due to thermal energy accumulation near the tabs or anywhere in the module.

Author declaration

We wish to confirm that there are no known conflicts of interest associated with this publication and there has been no financial support for this work that could have influenced its outcome.

We confirm that the manuscript has been read and approved by all named authors and that there are no other persons who satisfied the criteria for authorship but are not listed. We further confirm that the order of authors listed in the manuscript has been approved by all of us.

We confirm that we have given due consideration to the protection of intellectual property associated with this work and that there are no impediments to publication, including the timing of publication, with respect to intellectual property. In so doing we confirm that we have followed the regulations of our institutions concerning intellectual property.

We understand that the Corresponding Author is the sole contact for the Editorial process (including Editorial Manager and direct communications with the office). He is responsible for communicating with the other authors about progress, submissions of revisions and final approval of proofs. We confirm that we have provided a current, correct email address which is accessible by the Corresponding Author and which has been configured to accept email from the IJTF Journal.

Declaration of Competing Interest

It must be noted that at the time of submission, one of the authors was recently employed at Elsevier.

Acknowledgement

The financial support provided for this work by Innovative UK (Grant no. 3941/133371) is gratefully acknowledged.

References

[1] I. Tsiropoulos, N. Lebedeva, Li-ion batteries for mobility and stationary storage applications, (2018) 72. https://doi.org/10.2760/87175.
[2] Department of Transport, The Road to Zero Nukes, Dep. Tranport. (2018).
[3] H. Liu, Z. Wei, W. He, J. Zhao, Thermal issues about Li-ion batteries and recent progress in battery thermal management systems: a review, Energy Convers. Manag. 150 (2017) 304–330, https://doi.org/10.1016/j.enconman.2017.08.016.
[4] A.A. Pesaran, M. Keyser, G. Kim, S. Santhanagopalan, K. Smith, Tools for designing thermal management of batteries in electric drive vehicles battery temperature in xEVs, in: Adv. Automot. Batter. Conf., 2013, https://doi.org/10.2172/1064502.
[5] V. RUIZ RUIZ, P. Andreas, JRC exploratory research : Safer Li-ion batteries by preventing thermal propagation, 2018. https://doi.org/10.2760/096975.
[6] N. Sato, Thermal behavior analysis of lithium-ion batteries for electric and hybrid vehicles, J. Power Sources 99 (2001) 70–77, https://doi.org/10.1016/S0378-7753(01)00478-5.
[7] M. Broussely, P. Biensan, F. Bonhomme, P. Blanchard, S. Herreyre, K. Nechev, R. J. Staniewicz, Main aging mechanisms in Li ion batteries, J. Power Sources 146 (2005) 90–96, https://doi.org/10.1016/j.jpowsour.2005.03.172.
[8] G. Ning, B. Haran, B.N. Popov, Capacity fade study of lithium-ion batteries cycled at high discharge rates, J. Power Sources 117 (2003) 160–169, https://doi.org/10.1016/S0378-7753(03)00029-6.
[9] D.D. MacNeil, Z. Lu, Z. Chen, J.R. Dahn, A comparison of the electrode/electrolyte reaction at elevated temperatures for various Li-ion battery cathodes, J. Power Sources 108 (2002) 8–14, https://doi.org/10.1016/S0378-7753(01)01013-8.
[10] C.-K. Huang, J.S. Sakamoto, J. Wolfenstine, S. Surampudi, The limits of low-temperature performance of Li-ion cells, J. Electrochem. Soc. 147 (2000) 2893, https://doi.org/10.1149/1.1393622.
[11] H. -p. Lin, D. Chua, M. Salomon, H.-C. Shiao, M. Hendrickson, E. Plichta, S. Slane, Low-temperature behavior of Li-ion cells, Electrochem. Solid-State Lett. 4 (2001) A71, https://doi.org/10.1149/1.1368736.
[12] B. Wang, C. Ji, S. Wang, J. Sun, S. Pan, D. Wang, C. Liang, Study of non-uniform temperature and discharging distribution for lithium-ion battery modules in series and parallel connection, Appl. Therm. Eng. 168 (2020), 114831, https://doi.org/10.1016/j.applthermaleng.2019.114831.
[13] L.H. Saw, Y. Ye, A.A.O. Tay, Electro-thermal analysis and integration issues of lithium ion battery for electric vehicles, Appl. Energy. 131 (2014) 97–107, https://doi.org/10.1016/j.apenergy.2014.06.016.
[14] J. Liu, H. Li, W. Li, J. Shi, H. Wang, J. Chen, Thermal characteristics of power battery pack with liquid-based thermal management, Appl. Therm. Eng. 164 (2020), 114421, https://doi.org/10.1016/j.applthermaleng.2019.114421.
[15] S. Wiriyasart, C. Hommalee, S. Sirikasemsuk, R. Prurapark, P. Naphon, Thermal Management System with Nanofluids for Electric Vehicle, Case Stud. Therm. Eng. (2020), 100583, https://doi.org/10.1016/j.csite.2020.100583.
[16] J. He, X. Yang, G. Zhang, A phase change material with enhanced thermal conductivity and secondary heat dissipation capability by introducing a binary thermal conductive skeleton for battery thermal management, Appl. Therm. Eng. 148 (2019) 984–991, https://doi.org/10.1016/j.applthermaleng.2018.11.100.
[17] H. Jouhara, N. Khordehgah, S. Almahmoud, B. Delpech, A. Chauhan, S.A. Tassou, Waste heat recovery technologies and applications, Therm. Sci. Eng. Prog. 6 (2018) 268–289, https://doi.org/10.1016/J.TSEP.2018.04.017.
[18] Z. Zhang, K. Wei, Experimental and numerical study of a passive thermal management system using flat heat pipes for lithium-ion batteries, Appl. Therm. Eng. (2019), 114660, https://doi.org/10.1016/J.APPLTHERMALENG.2019.114660.
[19] Y. Gan, J. Wang, J. Liang, Z. Huang, M. Hu, Development of thermal equivalent circuit model of heat pipe-based thermal management system for a battery module with cylindrical cells, Appl. Therm. Eng. 164 (2020), 114523, https://doi.org/10.1016/j.applthermaleng.2019.114523.
[20] X. Yuan, A. Tang, C. Shan, Z. Liu, J. Li, Experimental investigation on thermal performance of a battery liquid cooling structure coupled with heat pipe, J. Energy Storage 32 (2020), 101984, https://doi.org/10.1016/j.est.2020.101984.
[21] M. Yao, Y. Gan, J. Liang, D. Dong, L. Ma, J. Liu, Q. Luo, Y. Li, Performance simulation of a heat pipe and refrigerant-based lithium-ion battery thermal management system coupled with electric vehicle air-conditioning, Appl. Therm. Eng. 191 (2021), 116878, https://doi.org/10.1016/j.applthermaleng.2021.116878.
[22] H. Behi, M. Behi, D. Karimi, J. Jaguemont, M. Ghanbarpour, M. Behnia, M. Berecibar, J. van Mierlo, Heat pipe air-cooled thermal management system for lithium-ion batteries: High power applications, Appl. Therm. Eng. 183 (2021), 116240, https://doi.org/10.1016/j.applthermaleng.2020.116240.
[23] A. Alihosseini, M. Shafaee, Experimental study and numerical simulation of a Lithium-ion battery thermal management system using a heat pipe, J. Energy Storage 39 (2021), 102616, https://doi.org/10.1016/j.est.2021.102616.
[24] H. Jouhara, N. Serey, N. Khordehgah, R. Bennett, S. Almahmoud, S.P. Lester, Investigation, development and experimental analyses of a heat pipe based battery thermal management system, Int. J. Thermofluids. (2019), 100004, https://doi.org/10.1016/j.ijft.2019.100004.